

The Interplanetary Network Supplement to the BATSE Catalogs of Untriggered Cosmic Gamma-Ray Bursts

K. Hurley¹

khurley@ssl.berkeley.edu

B. Stern^{2,3,4}

J. Kommers⁵

T. Cline⁶

E. Mazets, S. Golenetskii⁷

J. Trombka, T. McClanahan⁸

J. Goldsten⁹

M. Feroci¹⁰

F. Frontera^{11,12}

C. Guidorzi^{13,12}

E. Montanari¹²

W. Lewin¹⁴

C. Meegan, G. Fishman, C. Kouveliotou¹⁵

S. Sinha, S. Seetha,¹⁶

ABSTRACT

We present Interplanetary Network (IPN) detection and localization information for 211 gamma-ray bursts (GRBs) observed as untriggered events by the Burst and Transient Source Experiment (BATSE), and published in catalogs by Kommers et al. (2001) and Stern et al. (2001). IPN confirmations have been obtained by analyzing the data from 11 experiments. For any given burst observed by BATSE and one other distant spacecraft, arrival time analysis (or “triangulation”) results in an annulus of possible arrival directions whose half-width varies between 14 arcseconds and 5.6 degrees, depending on the intensity, time history, and arrival direction of the burst, as well as the distance between the spacecraft. This annulus generally intersects the BATSE error circle, resulting in a reduction of the area of up to a factor of ~ 650 . When three widely separated spacecraft observed a burst, the result is an error box whose area is as much as 30000 times

¹University of California, Berkeley, Space Sciences Laboratory, Berkeley, CA 94720-7450

²Institute for Nuclear Research, Russian Academy of Sciences, Moscow 117312, Russia.

³Astro Space Center of the Lebedev Physical Institute, Profsoyuznaya 84/32, Moscow 117810, Russia.

⁴SCFAB, Stockholm Observatory, SE-10691, Stockholm, Sweden

⁵MIT Lincoln Laboratory, Lexington, MA 02420-9108

⁶NASA Goddard Space Flight Center, Code 661, Greenbelt, MD 20771

⁷Ioffe Physico-Technical Institute, St. Petersburg, 194021, Russia

⁸NASA Goddard Space Flight Center, Code 691, Greenbelt, MD 20771

⁹The Johns Hopkins University, Applied Physics Laboratory, Laurel, MD 20723

¹⁰Istituto di Astrofisica Spaziale, C.N.R., Area di Ricerca Tor Vergata, Via Fosso del Cavaliere 100, 00133 Roma, Italy

¹¹Istituto Astrofisica Spaziale e Fisica Cosmica, C.N.R., Sezione di Bologna, Via Gobetti 101, 40129 Bologna, Italy

¹²Dipartimento di Fisica, Universita di Ferrara, Via Paradiso 12, 44100, Ferrara, Italy

¹³Astrophysics Research Institute, Liverpool John Moores University, Twelve Quays House, Egerton Wharf, Birkenhead CH41 1LD, United Kingdom

¹⁴Massachusetts Institute of Technology, Center for Space Research 37-627, Cambridge MA 02139

¹⁵NASA/MSFC, National Space Science and Technology Center, SD-50, 320 Sparkman Drive, Huntsville, AL 35805

¹⁶ISRO Satellite Center, Space Astronomy and Instrumentation Division, Bangalore 560 017, India

smaller than that of the BATSE error circle.

Because the IPN instruments are considerably less sensitive than BATSE, they generally did not detect the weakest untriggered bursts, but did detect the more intense ones which failed to trigger BATSE when the trigger was disabled. In a few cases, we have been able to identify the probable origin of bursts as soft gamma repeaters. The vast majority of the IPN-detected events, however, are GRBs, and the confirmation of them validates many of the procedures utilized to detect BATSE untriggered bursts.

Subject headings: gamma-rays: bursts; catalogs

1. Introduction

This paper presents the 8th catalog of gamma-ray burst (GRB) localizations obtained by arrival time analysis, or “triangulation” between the missions in the 3rd interplanetary network (IPN), which began operations in 1990 and continues to operate today. Two of these catalogs (Hurley et al. 1999a,b) were supplements to the BATSE 3B and 4Br burst catalogs (Meegan et al. 1996; Paciesas et al. 1999). The others involved bursts observed by numerous other spacecraft (Laros et al. 1997, 1998; Hurley et al., 2000a,b,c). In this paper, we present IPN data on 211 *untriggered* bursts which occurred throughout the entire *Compton Gamma-Ray Observatory (CGRO)* mission (1991 April through 2000 May). The BATSE data on these events, such as durations, fluxes, fluences, and coarse location information, appear in two catalogs, Kommers et al. (2001) and Stern et al. (2001). A final IPN supplement catalog, to the BATSE 5B catalog, is in preparation (Hurley et al. 2004, Briggs et al., 2004).

The purpose of searching the BATSE data for untriggered events was mainly to extend the number-intensity ($\log N$ - $\log S$) distribution to weaker bursts than those that could trigger the detector, and thus to gain more information on the burst distribution, particularly at the weak end. Other objectives included the detection of bursts from known and unknown soft gamma repeaters, and very soft transients which could constitute a previously unknown phenomenon. (One significant outcome of this effort was the detection of the bursting pulsar). The purpose of searching the IPN data for these events was to confirm as many of them as possible, reduce the sizes of their error circles, and validate the procedures used to identify these untriggered events.

2. Instrumentation, Search Procedure, Derivation of Annuli, and Burst Selection Criteria

We have used the same procedures as those employed in the other BATSE catalog supplements, and refer the reader to Hurley et al. (1999a,b) for the detailed descriptions. Generally speaking, using the arrival time and direction of a burst at BATSE, and its time history, we searched the data of the near-Earth spacecraft for a confirmation at the same time; for the spacecraft which were far from Earth, we searched for a confirmation (i.e., an event with a matching time history) in the appropriate crossing time window. Although more than 15 separate gamma-ray burst experiments were operating on over a dozen missions throughout the duration of the CGRO mission, confirmations were obtained from the data of just 11 experiments: the *BeppoSAX* Gamma-Ray Burst Monitor (Frontera et al. 1997; Feroci et al. 1997), the *Defense Meteorological Satellite Program* (DMSP, Terrell et al. 1992), Ginga (Murakami et al. 1989), Konus-A (Aptekar et al. 1997), Konus - *Wind* (Aptekar et al. 1992), the Near Earth Asteroid Rendezvous mission (NEAR, Goldsten et al. 1997), PHEBUS (Terekhov et al. 1994), *Pioneer Venus Orbiter* (Klebesadel et al. 1980), SROSS C-2 (Kasturirangan et al. 1997), *Ulysses* (Hurley et al. 1992), and WATCH - GRANAT (Brandt, Lund, & Rao 1990). We note here, however, two important differences in the procedures and results between the triggered and untriggered events.

First, the untriggered burst catalogs contain a much higher proportion of weak events than the BATSE triggered burst catalogs. Because the IPN instruments are generally much less sensitive than BATSE, they detected a smaller fraction of the untriggered than the triggered ones.

Second, the untriggered event time histories were recorded in the 1.024 s resolution BATSE data, while the triggered event time histories were recorded with much higher time resolution. Thus when an untriggered event was detected only by BATSE and another near-Earth spacecraft, the low time resolution and the proximity of the two spacecraft results in a very wide annulus which is consistent with, but does not constrain the BATSE error circle. Twenty-one events fell into this category, and it is only possible to confirm their detection, but not to obtain a meaningful annulus or error box for them.

3. A Few Statistics

There are 873 untriggered bursts in the Kommers et al. (2001) catalog and 1838 untriggered bursts in the Stern et al. (2001) catalog. The two sets are not mutually exclusive (Stern et al. 2001), and the total number of untriggered bursts is approximately 2000, de-

pending on the exact acceptance criteria. Their peak fluxes range from 0.06 to 25 photons $\text{cm}^{-2} \text{s}^{-1}$. Figure 1 gives the IPN efficiency for detecting untriggered bursts as a function of their peak fluxes. This is defined as the number of bursts detected by the IPN divided by the total number of untriggered bursts in a particular flux range. There are many factors which determine whether a burst is detected by an IPN spacecraft. In addition to the burst intensity and time history, solar activity, Earth-blocking for spacecraft in low Earth orbit, the number of spacecraft active in the IPN, and data return all play important, time-variable roles. Figure 1 therefore gives time-averaged efficiencies. Approximately one out of nine untriggered BATSE bursts was observed by at least one spacecraft in the IPN. Their fluxes range from 0.15 to 25 photons $\text{cm}^{-2} \text{s}^{-1}$. For comparison, approximately one out of every three triggered BATSE bursts was observed by IPN spacecraft (Hurley et al. 1999b). Of the 211 IPN events, only 90 could be localized (85 to annuli only, and 5 to error boxes).

4. Tables of Confirmed Bursts, Annuli, and Error Boxes

For each confirmed untriggered burst, table 1 lists the spacecraft which observed the event. (A list of *all* GRBs and the IPN spacecraft which detected them may be found at <http://ssl.berkeley.edu/ipn3/masterli.html> or <http://heasarc.gsfc.nasa.gov/W3Browse/>.)

For those bursts which can be localized, either to a single annulus whose width is comparable to or less than the diameter of the BATSE error circle (an example is shown in figure 2), or to an error box (an example is shown in figure 3), the 6 columns in table 2 give:

1) the date of the burst, in yyymmdd format, 2) the Universal Time of the burst at Earth in seconds, 3) the right ascension of the center of the IPN annulus, epoch J2000, in the heliocentric frame, in degrees, 4) the declination of the center of the IPN annulus, epoch J2000, in the heliocentric frame, in degrees, 5) the angular radius R_{IPN1} of the first IPN annulus, in the heliocentric frame, in degrees, and 6) the half-width δR_{IPN1} of the first IPN annulus, in degrees; the 3σ confidence annulus is given by $R_{IPN1} \pm \delta R_{IPN1}$.

If the burst was detected by a third, distant spacecraft, and a non-degenerate second annulus could be derived for it, the information in columns 4, 5, and 6 is repeated for this annulus.

For the bursts in table 2, table 3 gives the BATSE error circles, from Kommers et al. (2001) and Stern et al. (2001), and either a) the intersection points of the IPN annulus with the error circle, or b) for the three-spacecraft localizations, the four corners of the IPN error box.

For each entry, the first line contains:

1) the date of the burst, in yymmdd format, 2) the Universal Time of the burst at Earth, in seconds, 3) the right ascension of the center of the BATSE error circle, in degrees, 4) the declination of the center of the BATSE error circle, in degrees, and 5) the radius of the BATSE error circle, in degrees; this is the combination of the one sigma statistical error and a 1.6 degree systematic error, summed in quadrature.

The four following lines contain the right ascension and declination, in degrees, of the error box. For those bursts which were observed by BATSE and a single IPN spacecraft (e.g. figure 2), the coordinates are those of the intersection of the 3σ IPN annulus with the 1σ (statistical plus systematic) BATSE error circle. Although all of the annuli are statistically consistent with the positions of their respective 1σ BATSE error circles, in some cases part or all of the annulus does not actually intersect the error circle. In those cases, the coordinates are set to zero. For those bursts which were observed by two distant IPN spacecraft (e.g. figure 2), and for which an IPN-only error box can be derived, the coordinates given are those of the IPN error box.

All coordinates are J2000, and all event times are the ones used to identify the bursts in the Stern et al. (2001) and Kommers et al. (2001) catalogs.

5. Notes on specific events

We note here a number of unusual circumstances surrounding some of the bursts in the Stern et al. (2001) and Kommers et al. (2001) catalogs.

- Some of the bursts in the two catalogs in fact correspond to BATSE triggers. In some cases, the triggers were not caused by the bursts, but the bursts were nevertheless recorded in triggered mode.
- The Kommers et al. (2001) catalog was divided into two parts: high energy (HE) events, and low energy (LE) events. Initially, there were 125 LE events, but 75 of them were intentionally eliminated from the final catalog because their origin was suspected to be either magnetospheric, X-ray binaries in outburst, or activity from soft gamma repeaters (SGRs). We have identified four of the 75 eliminated events as bursts from SGR1806-20. These four can be found in the complete list of SGR bursts identified in the Kommers et al. (2001) search, available at <http://space.mit.edu/BATSE/data.html>.
- A total of 9 of the untriggered events probably originated from soft gamma repeaters. In some cases, they had in fact triggered BATSE and were recorded in triggered mode.

The IPN localizations of these SGR bursts serve as a good calibration of the techniques and data used here, however. They verify, for example, that the 1 s resolution BATSE data files in the Stern et al. (2001) and Kommers et al. (2001) catalogs have the correct timing, and that the localization procedures used in these catalogs, and by the IPN, are accurate.

The following list gives the details.

GRB920903, 05728 s. This burst was observed by WATCH-GRANAT (Sazonov et al. 1995). Both the Ulysses/WATCH and Ulysses/BATSE annuli are consistent with the WATCH error circle, but do not intersect the BATSE error circle. The BATSE error circle lies ~ 7 degrees away from the WATCH error circle, but is consistent with it, given the statistical and systematic uncertainties. The intersection of the narrower Ulysses/BATSE annulus with the WATCH error circle is given here.

GRB920920, 04415 s. This event was recorded in triggered mode following BATSE trigger 1948. The trigger occurred due to a different GRB.

GRB930209, 15737 s. This event was recorded in triggered mode following BATSE trigger 2177. The trigger occurred due to a solar flare.

GRB930702, 68333 s. This burst corresponds to BATSE trigger 2426, which is believed to be a Cygnus X-1 fluctuation.

GRB931005, 82288 s. This burst is a Kommers et al. (2001) LE event which was eliminated from the final catalog. It is BATSE trigger 2565, from SGR1806-20.

GRB940710, 35477 s. This event occurred 251 s before BATSE trigger 3071, whose duration is T90=71 s. The location of the Kommers et al. (2001) event is RA, Decl. = 99.4° , -33.3° , with uncertainty 3.4° , and that of BATSE 3071 is RA, Decl. = 96.42° , -36.59° , with uncertainty 1.33° . The centers of the two circles are therefore 4.1° apart. The IPN annulus is consistent with both error circles. Thus the Kommers et al. (2001) event may be a precursor to 3071.

GRB950730, 76147 s. This event corresponds to BATSE trigger 3720, which was due to a Cygnus X-1 fluctuation. The burst occurred 25 s after the trigger.

GRB950904, 52777 s. This event occurred about 75 s after BATSE trigger 3776. Its duration is given as 108 s in Stern et al. (2001), but this duration included the triggered event, which is unrelated to it. The correct duration is ~ 30 s.

GRB961119, 21322 s. This burst is a Kommers et al. (2001) LE event which was eliminated from the final catalog. The IPN annulus is consistent with the position of SGR1806-20.

GRB961119, 21536 s. This burst is a Kommers et al. (2001) LE event which was eliminated from the final catalog. It is probably from SGR1806-20, but it cannot be triangulated with any precision.

GRB961119, 26961 s. This burst is a Kommers et al. (2001) LE event which was eliminated from the final catalog. It is probably from SGR1806-20, but it cannot be triangulated with any precision.

GRB980622, 51085 s. This event is BATSE trigger 6861. It originates from SGR1627-41.

GRB980728, 64911 s. This event is BATSE trigger 6954. It originates from SGR1627-41.

GRB980801, 12920 s. This event is BATSE trigger 6959. It originates from SGR1627-41.

GRB980913 at 19983 s. This is BATSE trigger 7087.

GRB981022, 56447 s. This event is BATSE trigger 7171, from SGR1900+14.

GRB990110, 31141 s. This is BATSE trigger 7315. This burst originates from SGR1900+14.

GRB990429, 35555 s. This event is BATSE trigger 7536. It originates from SGR1900+14.

GRB990507, 71334 s. This is BATSE trigger 7552.

GRB991101, 54480 s. This is BATSE trigger 7835. It is probably a GRB observed with particle contamination.

6. Discussion and Conclusion

The Kommers et al. (2001) and Stern et al. (2001) studies of untriggered BATSE bursts pointed to different conclusions about the GRB population. The sample of Stern et al. provides evidence for a GRB number-intensity relation which continues to increase at low intensities, while the sample of Kommers et al. provides evidence for a flattening. The analysis which we have presented here indicates only that many of the events with peak fluxes above ~ 0.15 photon cm^{-2} s^{-1} are likely to be real, and that relatively few of them have been misclassified. The likelihood of reality increases with peak flux (figure 1). As there are hundreds of untriggered bursts below the IPN threshold, the possibility exists that the different conclusions about the number-intensity relation are due to the differences in classifying weak untriggered events. A recent study of untriggered BATSE bursts by Mitrofanov et al. (2004) reinforces and quantifies this idea. While this study is a preliminary one and does not draw any conclusions about the weak events, it should eventually lead to a clearer classification of them. A definitive statement about the weak burst population may

also be forthcoming after the launch of the Swift mission (Gehrels et al. 2004).

7. Acknowledgments

Support for the *Ulysses* GRB experiment is provided by JPL Contract 958056. Joint analysis of *Ulysses* and BATSE data was supported by NASA Grants NAG 5-1560 and NAG5-9701. NEAR data analysis was supported under NASA Grants NAG 5-3500 and NAG 5-9503. We are also grateful to the NEAR team for their modifications to the XGRS experiment which made gamma-ray burst detection possible. The Konus-Wind experiment was supported by Russian Space Agency Contract and RBRF grant #03-02-17517.

REFERENCES

- Aptekar, R., et al. 1992, in AIP Conf. Proc. 265, Gamma-Ray Bursts, ed. W. Paciesas and G. Fishman (New York: AIP), 359
- Aptekar, R., et al. 1997, Astron. Lett. 23(2), 147
- Brandt, S., Lund, N., and Rao, A. 1990, Adv. Space Res. 10(2), 239
- Briggs, M., et al., 2004, in preparation
- Feroci, M., et al., 1997, in X-Ray, and Gamma-Ray Instrumentation for Astronomy VIII, Eds. O. Siegmund and M. Gummin, SPIE Vol. 3114, 186
- Frontera, F., et al. 1997, A&AS 122, 357
- Gehrels, N., et al. 2004, ApJ 611, 1005
- Goldsten, J., et al. 1997, Space Sci. Rev. 82(1/2), 169
- Guidorzi, C., et al. 2004, in preparation
- Hurley, K., et al. 1992, A&AS 92, 401
- Hurley, K., et al. 1999a, ApJS 120, 399
- Hurley, K., et al. 1999b, ApJS 122, 497
- Hurley, K., et al. 2000a, ApJ 533, 884
- Hurley, K., et al. 2000b, ApJ 534, 258
- Hurley, K., et al. 2000c, ApJS 128, 549
- Hurley, K., et al. 2004, in preparation
- Kasturirangan, K., Padmini, V. N., Prasad, N. L., Rao, U. R., and Seetha, S. 1997, A&A 322, 778
- Klebesadel, R., et al. 1980, IEEE Trans. on Geoscience and Remote Sensing, GE-18, 1
- Kommers, J., Lewin, W., Kouveliotou, C., van Paradijs, J., Pendleton, G., Meegan, C., and Fishman, G., 2001, ApJS 134, 385
- Laros, J., et al. 1997, ApJS 110, 157
- Laros, J., et al. 1998, ApJS 118, 391
- Meegan, C., et al., 1996, ApJS 106, 65
- Mitrofanov, I., et al. 2004, ApJ 603, 624
- Murakami, T., et al. 1989, PASJ 41, 405
- Paciesas, W., et al. 1999, ApJS 122, 465

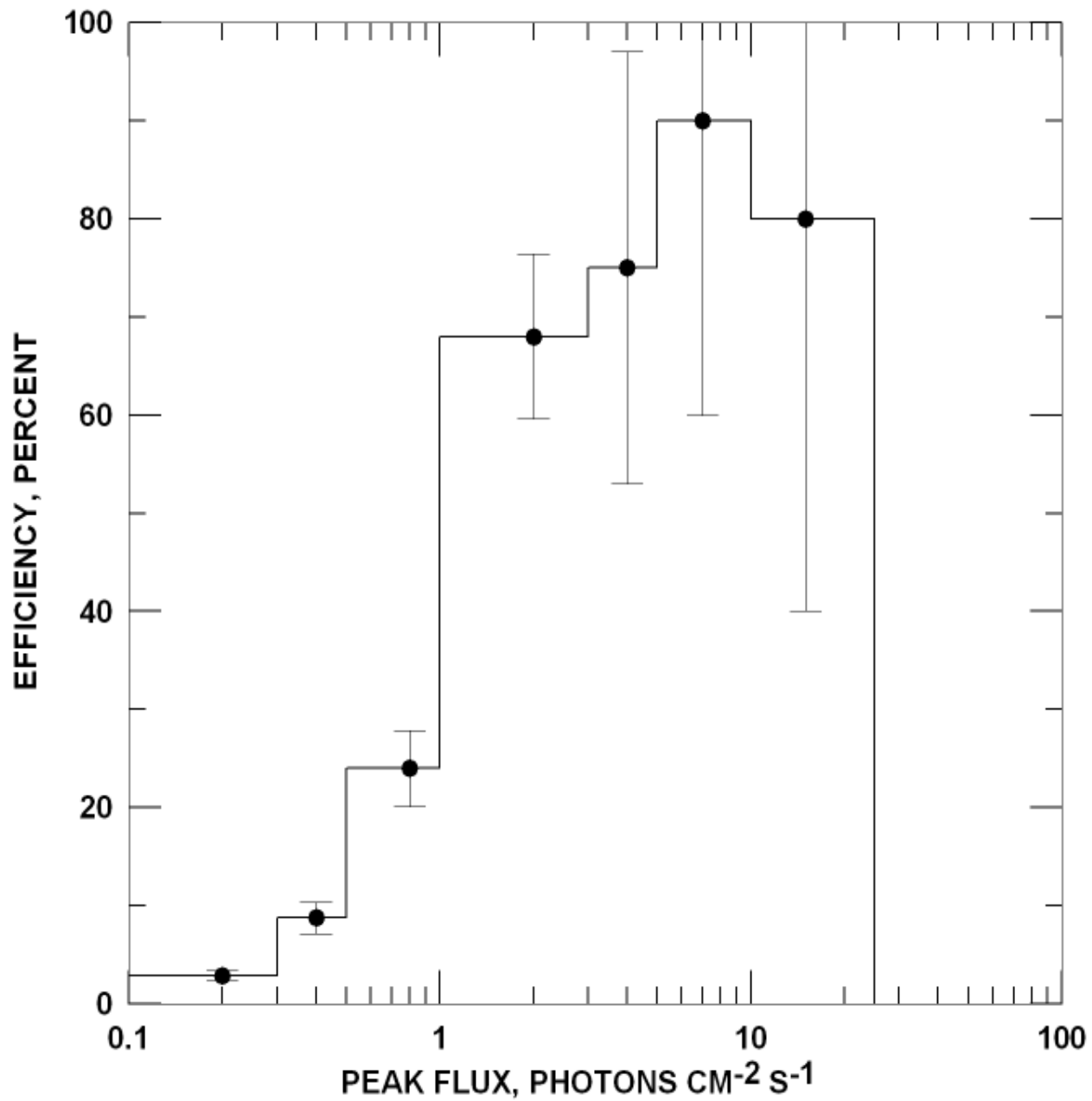
- Piro, L., & Costa, E. 1998, GCN Circ. 99
- Sazonov, S., Sunyaev, R., Terekhov, O., Lund, N., Brandt, S., and Castro-Tirado, A. 1998, A&AS 129, 1
- Stern, B., Tikhomirova, Y., Kompaneets, D., Svensson, R., and Poutanen, J., 2001, ApJ 563, 80
- Terekhov, O., et al. 1994, Astron. Lett. 20(3), 265
- Terrell, J., Klebesadel, R., Lee, P., and Griffee, J. 1992, in AIP Conf. Proc. 265, Gamma-Ray Bursts, ed. W. Paciesas and G. Fishman (New York: AIP), 48
- Tkachenko, A., et al. 1998, Astron. Lett. 24(6), 722

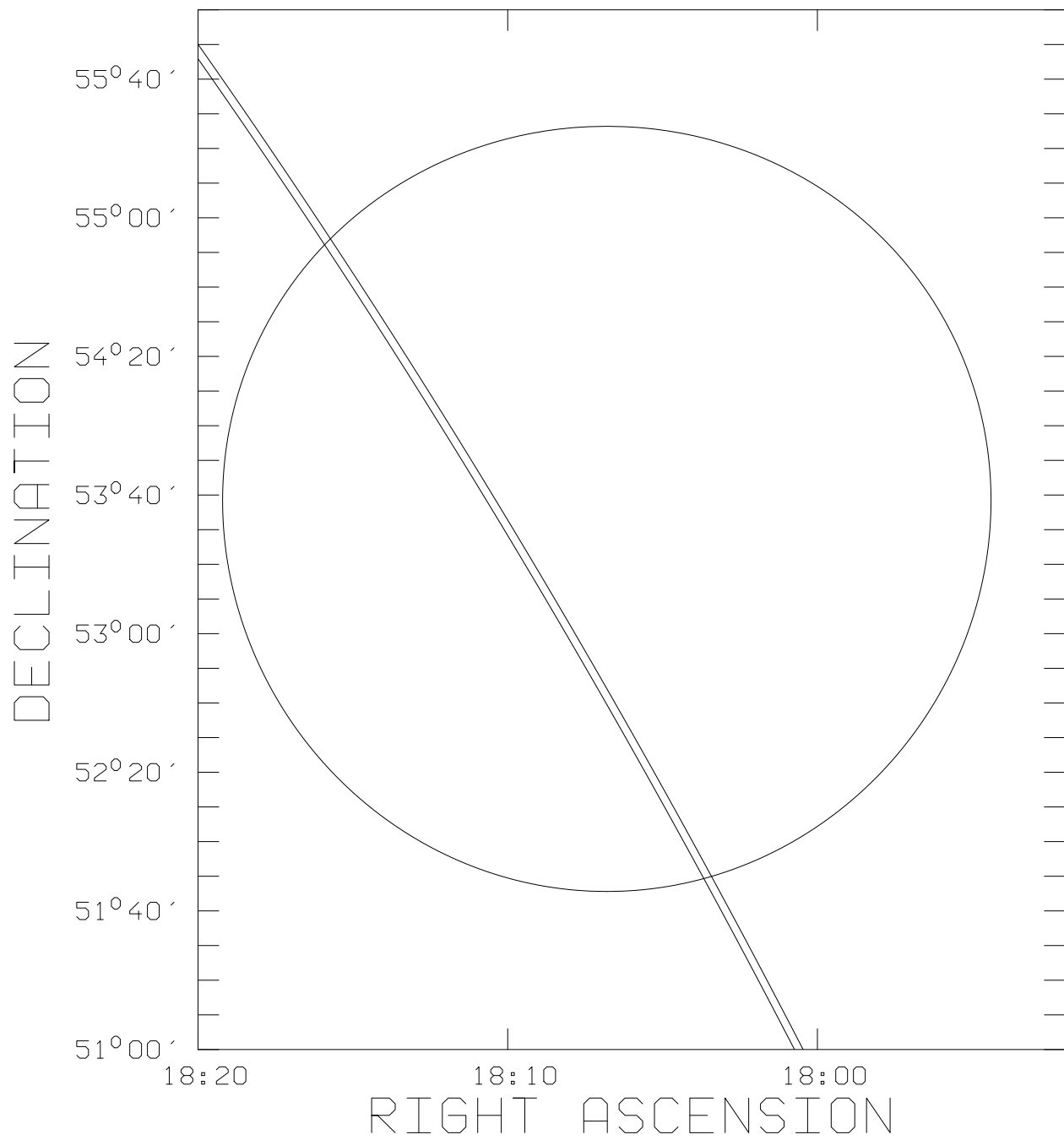
FIGURE CAPTIONS

Fig. 1.— The IPN efficiency for detecting a BATSE untriggered burst. This is the number of bursts in a flux range detected by the IPN, divided by the number detected by BATSE. The peak fluxes of the untriggered bursts range from 0.06 to 25 photons cm⁻² s⁻¹. The efficiencies are time-averaged.

Fig. 2.— The BATSE 1σ (statistical + systematic) error circle for the untriggered event on 980629, and the 3σ IPN annulus. Note that in general the curvature of the annulus makes it impossible to describe the resulting error box with only the four annulus/error circle intersection points.

Fig. 3.— The BATSE 1σ (statistical + systematic) error circle for the untriggered event on 000403, and the 3σ IPN error box, formed by the intersection of the two annuli.





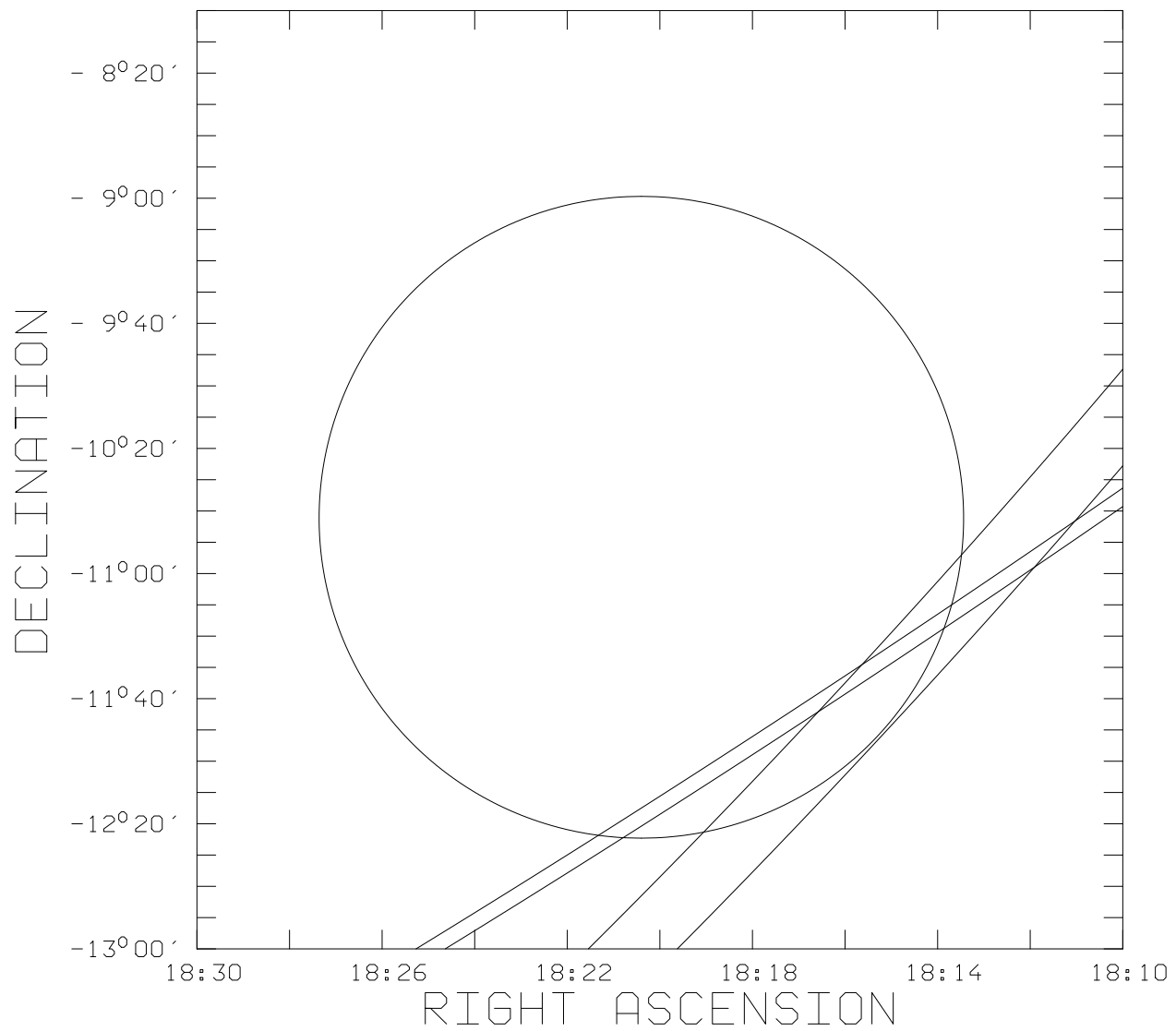


Table 1. BATSE untriggered bursts confirmed by the IPN

Date	UT	IPN spacecraft
910601	62220	<i>Ulysses</i>
910830	05148	<i>Ulysses</i>
910908	33924	<i>Ulysses</i>
910910	14747	<i>Ulysses</i>
911029	17453	<i>Ulysses</i> , PVO ^a , Ginga ^b
911120	43957	<i>Ulysses</i>
920109	23306	<i>Ulysses</i>
920216	58688	<i>Ulysses</i>
920303	24523	<i>Ulysses</i>
920622	23828	<i>Ulysses</i>
920626	64276	<i>Ulysses</i>
920717	57852	<i>Ulysses</i>
920903 ^c	05728	<i>Ulysses</i> , WATCH/GRANAT ^d
930118	64426	<i>Ulysses</i>
930209 ^c	15737	<i>Ulysses</i> , PHEBUS ^e
930408	06847	PHEBUS ^e
930424	38888	<i>Ulysses</i>
930506	55245	<i>Ulysses</i>
930626	07023	<i>Ulysses</i>
930710	13810	<i>Ulysses</i>
930909	45100	<i>Ulysses</i>
940213	07260	<i>Ulysses</i>
940222	08083	<i>Ulysses</i>
940311	44967	<i>Ulysses</i>
940710 ^c	35477	<i>Ulysses</i>
940712	00070	<i>Ulysses</i>
940727	40865	<i>Ulysses</i>
940730	39690	<i>Ulysses</i> , DMSP ^f , SROSS-C
940930	23017	<i>Ulysses</i>
941104	35178	<i>Ulysses</i>
950104	32438	Konus- <i>Wind</i>

Table 1—Continued

Date	UT	IPN spacecraft
950111	46528	<i>Ulysses</i>
950131	78592	<i>Ulysses, Konus-Wind</i>
950203	08456	<i>Ulysses, SROSS-C</i>
950207	72568	<i>Konus-Wind</i>
950211	15919	<i>Ulysses, Konus-Wind</i>
950224	33800	<i>Konus-Wind</i>
950603	21257	<i>Konus-Wind</i>
950611	21122	<i>Ulysses</i>
950614	00779	<i>Konus-Wind</i>
950615	12104	<i>Ulysses</i>
950622	71470	<i>Ulysses, Konus-Wind</i>
950625	09685	<i>Konus-Wind</i>
950722	64127	<i>Ulysses, Konus-Wind</i>
950723	73608	<i>Konus-Wind</i>
950728	45743	<i>Konus-Wind</i>
950730 ^c	76147	<i>Ulysses, Konus-Wind</i>
950904 ^c	52777	<i>Ulysses</i>
951001	41868	<i>Ulysses, Konus-Wind</i>
951005	14826	<i>Konus-Wind</i>
951013	57096	<i>Konus-Wind</i>
951112	67850	<i>Ulysses</i>
951124	25132	<i>Ulysses, Konus-Wind</i>
951213	32675	<i>Konus-Wind</i>
951215	73379	<i>Konus-Wind</i>
951218	28745	<i>Ulysses, Konus-Wind</i>
951231	77068	<i>Konus-Wind</i>
960107	68607	<i>Konus-Wind</i>
960115	31956	<i>Ulysses, Konus-Wind</i>
960123	43643	<i>Konus-Wind</i>
960201	82195	<i>Ulysses</i>
960202	05968	<i>Ulysses, Konus-Wind</i>

Table 1—Continued

Date	UT	IPN spacecraft
960207	65033	<i>Ulysses</i> , Konus- <i>Wind</i>
960304	48776	<i>Ulysses</i>
960321	19663	Konus- <i>Wind</i>
960418	08267	Konus- <i>Wind</i>
960504	18779	Konus- <i>Wind</i>
960602	42667	Konus- <i>Wind</i>
960603	60930	Konus- <i>Wind</i>
960614	83621	Konus- <i>Wind</i>
960715	58326	Konus- <i>Wind</i>
960725	63535	<i>BeppoSAX</i> ^g
960817	24647	Konus- <i>Wind</i>
960826	58072	Konus- <i>Wind</i>
960905	02568	Konus- <i>Wind</i>
961017	23648	<i>Ulysses</i>
961023	07747	<i>BeppoSAX</i> ^g
961106	43031	<i>BeppoSAX</i> ^g
961107	12691	Konus- <i>Wind</i>
961110	26976	Konus- <i>Wind</i> , <i>BeppoSAX</i> ^g
961113	80523	Konus- <i>Wind</i>
961119 ^c	21322	<i>Ulysses</i> , Konus- <i>Wind</i>
961119 ^c	21536	Konus-A
961119 ^c	26961	Konus-A
961120	30433	<i>BeppoSAX</i> ^g
961123	59316	Konus- <i>Wind</i>
961208	68232	<i>BeppoSAX</i> ^g
961209	74677	<i>Ulysses</i>
961213	49966	<i>Ulysses</i> , Konus- <i>Wind</i>
961222	43207	<i>BeppoSAX</i> ^g
961224	36648	Konus- <i>Wind</i> , <i>BeppoSAX</i> ^g
970116	58238	<i>Ulysses</i> , Konus- <i>Wind</i>
970119	42607	Konus- <i>Wind</i>

Table 1—Continued

Date	UT	IPN spacecraft
970221	13750	<i>BeppoSAX^g</i>
970223	64885	<i>BeppoSAX^g</i>
970311	30254	<i>BeppoSAX^g</i>
970406	25471	<i>Ulysses, Konus-Wind, BeppoSAX^g</i>
970525	31783	<i>BeppoSAX^g</i>
970610	36151	<i>BeppoSAX^g</i>
970617	61459	<i>BeppoSAX^g</i>
970720	68515	Konus- <i>Wind</i>
970801	29048	<i>Ulysses, Konus-Wind</i>
970817	69692	<i>BeppoSAX^g</i>
970825	40632	<i>BeppoSAX^g</i>
970827	25872	<i>BeppoSAX^g</i>
970926	79655	Konus- <i>Wind</i>
971015	20356	Konus- <i>Wind</i>
971017	01897	Konus- <i>Wind</i>
971019	57427	Konus- <i>Wind</i>
971027	09808	<i>Ulysses, BeppoSAX^g</i>
971028	75126	<i>BeppoSAX^g</i>
971101	23483	<i>Ulysses, Konus-Wind</i>
971102	05581	<i>BeppoSAX^g</i>
971103	27090	<i>BeppoSAX^g</i>
971121	43992	<i>Ulysses, Konus-Wind</i>
971207	67900	<i>Ulysses, Konus-Wind</i>
971207	75492	<i>Ulysses, BeppoSAX^g</i>
971228	53605	<i>BeppoSAX^g</i>
971228	79012	Konus- <i>Wind</i> , NEAR
980106	44231	Konus- <i>Wind</i>
980205	19783	<i>Ulysses, Konus-Wind, BeppoSAX^g, NEAR</i>
980207	58212	Konus- <i>Wind</i>
980223	76640	<i>BeppoSAX^g</i>
980226	41332	<i>BeppoSAX^g</i>

Table 1—Continued

Date	UT	IPN spacecraft
980304	52863	Konus- <i>Wind</i> , <i>BeppoSAX</i> ^g
980329	55486	<i>BeppoSAX</i> ^g
980429	20493	Konus- <i>Wind</i>
980518	67488	<i>BeppoSAX</i> ^g
980520	52002	<i>BeppoSAX</i> ^g
980523	31208	<i>Ulysses</i> , Konus- <i>Wind</i>
980602	46528	Konus- <i>Wind</i>
980605	51131	Konus- <i>Wind</i> , <i>BeppoSAX</i> ^g
980613	17465	<i>BeppoSAX</i> ^h
980622 ^c	51085	<i>Ulysses</i>
980626	70184	Konus- <i>Wind</i>
980629	32377	<i>Ulysses</i> , Konus- <i>Wind</i>
980705	23165	<i>BeppoSAX</i> ^g
980706	63987	Konus- <i>Wind</i> , <i>BeppoSAX</i> ^g
980709	16963	<i>BeppoSAX</i> ^g
980712	18577	<i>BeppoSAX</i> ^g
980713	13301	Konus- <i>Wind</i> , <i>BeppoSAX</i> ^g
980715	35282	<i>BeppoSAX</i> ^g
980728	53879	Konus- <i>Wind</i>
980728	55355	Konus- <i>Wind</i>
980808	78791	<i>BeppoSAX</i> ^g
980810	15944	<i>BeppoSAX</i> ^g
980812	17640	<i>BeppoSAX</i> ^g
980812	18950	<i>Ulysses</i> , Konus- <i>Wind</i> , <i>BeppoSAX</i> ^g
980907	40388	<i>BeppoSAX</i> ^g
980908	02480	<i>BeppoSAX</i> ^g
980913 ^c	19983	<i>Ulysses</i> , NEAR
980916	73322	<i>BeppoSAX</i> ^g
980917	35279	<i>BeppoSAX</i> ^g
980923	30178	<i>BeppoSAX</i> ^g
981002	05466	<i>BeppoSAX</i> ^g

Table 1—Continued

Date	UT	IPN spacecraft
981018	01612	<i>BeppoSAX^g</i>
981019	79603	<i>Ulysses</i> , Konus- <i>Wind</i> , <i>BeppoSAX^g</i>
981022	21682	<i>BeppoSAX^g</i>
981022 ^c	56447	<i>Ulysses</i> , Konus- <i>Wind</i>
981101	26940	<i>Ulysses</i> , Konus- <i>Wind</i> , NEAR
981106	38479	<i>BeppoSAX^g</i>
981215	80709	Konus- <i>Wind</i> , NEAR
981216	19755	<i>BeppoSAX^g</i>
990104	39597	<i>BeppoSAX^g</i>
990109	41054	<i>Ulysses</i> , Konus- <i>Wind</i>
990110 ^c	31141	<i>Ulysses</i>
990128	37252	<i>Ulysses</i> , Konus- <i>Wind</i> , <i>BeppoSAX^g</i>
990204	30169	<i>Ulysses</i> , Konus- <i>Wind</i>
990305	34451	Konus- <i>Wind</i>
990421	65775	<i>Ulysses</i>
990504	40929	<i>BeppoSAX^g</i>
990509	74345	<i>Ulysses</i>
990526	47273	<i>BeppoSAX^g</i>
990603	66686	<i>BeppoSAX^g</i>
990606	11124	Konus- <i>Wind</i>
990618	37636	<i>BeppoSAX^g</i>
990621	43943	<i>BeppoSAX^g</i>
990705	57685	<i>Ulysses</i> , Konus- <i>Wind</i> , <i>BeppoSAX^g</i> , NEAR
990707	54801	<i>Ulysses</i> , Konus- <i>Wind</i> , <i>BeppoSAX^g</i>
990711	49110	<i>BeppoSAX^g</i>
990719	79380	<i>BeppoSAX^g</i>
990720	00025	<i>BeppoSAX^g</i>
990725	41016	<i>BeppoSAX^g</i>
990727	48288	<i>BeppoSAX^g</i>
990803	57565	<i>BeppoSAX^g</i>
990806	60168	Konus- <i>Wind</i>

Table 1—Continued

Date	UT	IPN spacecraft
990828	70019	<i>Ulysses</i> , Konus- <i>Wind</i>
990917	52494	<i>BeppoSAX</i> ^g
990917	71095	<i>BeppoSAX</i> ^g
990919	49338	Konus- <i>Wind</i> , <i>BeppoSAX</i> ^g , NEAR
990919	86038	Konus- <i>Wind</i>
990926	32653	NEAR
991002	15031	<i>BeppoSAX</i> ^g
991004	22825	<i>BeppoSAX</i> ^g
991005	15265	<i>Ulysses</i>
991011	35968	Konus- <i>Wind</i> , <i>BeppoSAX</i> ^g
991120	27069	NEAR
991205	82651	<i>BeppoSAX</i> ^g
991217	21782	<i>BeppoSAX</i> ^g
000102	27709	<i>Ulysses</i>
000205	45486	<i>Ulysses</i> , <i>BeppoSAX</i> ^g
000206	09183	<i>Ulysses</i> , <i>BeppoSAX</i> ^g
000210	14030	Konus- <i>Wind</i>
000211	45217	<i>BeppoSAX</i> ^g
000224	82209	<i>BeppoSAX</i> ^g
000318	12931	Konus- <i>Wind</i>
000403	13199	<i>Ulysses</i> , Konus- <i>Wind</i> , NEAR
000405	77386	<i>Ulysses</i>
000420	61374	<i>Ulysses</i> , Konus- <i>Wind</i>
000502	54060	<i>BeppoSAX</i> ^g
000511	66298	<i>Ulysses</i> , Konus- <i>Wind</i>

^aJ. Laros, private communication, 1991^bT. Murakami, private communication, 1991^cSee section 5

^dSazonov et al. 1998

^eTkachenko et al. 1998

^fJ. Terrell, private communication, 1995

^gGuidorzi et al. 2004

^hPiro & Costa 1998

Table 2. *IPN annuli*

Date	UT	$\alpha_{2000, IPN}$	$\delta_{2000, IPN}$	R_{IPN1}	δR_{IPN}
910601	62220	307.008	-20.544	31.555	0.602
910830	05148	152.409	12.566	48.690	0.306
910908	33924	154.638	11.730	84.755	0.092
910910	14747	155.049	11.574	19.634	0.072
911029	17453	344.478	-7.880	29.352	0.050
911120	43957	167.141	6.825	86.994	0.049
920109	23306	347.750	-6.711	47.721	0.173
920216	58688	342.389	-8.336	32.244	0.135
920303	24523	338.881	-8.709	21.076	0.083
920622	23828	150.168	6.668	48.411	0.135
920626	64276	330.525	-6.378	65.379	0.045
920717	57852	152.612	4.858	77.394	0.050
920903	05728	338.736	-0.545	54.228	0.063
930118	64426	163.857	-13.874	54.969	0.035
930209	15737	159.547	-14.829	70.983	0.050
930424	38888	144.212	-12.262	78.603	0.549
930506	55245	323.364	11.717	66.872	0.992
930626	07023	325.198	11.491	67.667	0.374
930710	13810	326.814	12.090	82.054	0.024
930909	45100	336.355	17.978	87.746	0.038
940213	07260	151.385	-51.418	39.877	0.189
940222	08083	146.406	-52.260	86.434	0.118
940311	44967	136.417	-52.192	85.580	0.439
940710	35477	128.502	-39.575	25.746	0.750
940712	00070	128.902	-39.677	44.911	0.058
940727	40865	313.160	41.197	47.661	0.206
940730	39690	134.062	-41.599	35.990	0.072
940930	23017	341.171	58.806	65.096	0.510
941104	35178	26.375	73.600	57.376	0.187
950111	46528	322.648	-44.901	66.079	0.119
950131	78592	331.984	-31.567	29.273	0.527

Table 2—Continued

Date	UT	$\alpha_{2000,IPN}$	$\delta_{2000,IPN}$	R_{IPN1}	δR_{IPN}
950203	08456	332.839	-30.167	89.992	0.030
950211	15919	335.834	-25.077	30.200	0.130
950611	21122	196.445	-57.824	26.966	1.033
950615	12104	198.715	-60.874	56.631	0.518
950622	71470	204.112	-66.756	68.801	0.141
950722	64127	98.551	83.396	57.905	0.379
950730	76147	320.422	-82.230	77.858	0.039
950904	52777	190.636	67.767	36.463	0.144
951001	41868	202.666	60.024	80.559	0.068
951112	67850	216.222	54.930	39.289	0.202
951124	25132	219.201	55.029	38.194	1.044
951218	28745	44.049	-57.317	39.343	0.089
960115	31956	45.389	-63.277	45.746	0.090
960201	82195	41.130	-68.152	88.655	0.146
960202	05968	221.086	68.185	49.051	0.164
960207	65033	218.206	69.749	73.961	0.089
960304	48776	192.220	74.434	75.937	0.404
961017	23648	174.945	32.043	15.768	0.302
961209	74677	179.842	31.294	2.542	5.564
961213	49966	179.845	31.446	24.486	0.129
970116	58238	176.897	33.808	84.760	0.143
970406	25471	335.943	-35.323	42.658	0.277
970801	29048	337.672	-22.111	38.624	0.222
971027	09808	169.177	13.952	58.403	0.013
971101	23483	349.656	-13.606	27.793	0.014
971121	43992	351.033	-12.487	73.989	0.115
971207	67900	171.412	11.889	75.290	0.226
971207	75492	171.412	11.887	62.197	0.051
971228	79012	83.395	20.899	81.666	2.305
980205	19783	165.363	12.132	53.914	0.040
		183.317	-72.020	38.790	2.212

Table 2—Continued

Date	UT	$\alpha_{2000,IPN}$	$\delta_{2000,IPN}$	R_{IPN1}	δR_{IPN}
980523	31208	329.478	-11.682	36.270	0.183
980622	51085	330.752	-9.840	77.221	0.029
980629	32377	331.305	-9.351	80.020	0.019
980812	18950	336.276	-5.670	38.173	0.061
980913	19983	340.559	-2.546	31.980	0.278
		67.928	25.235	56.955	0.483
981019	79603	344.985	1.273	45.039	0.029
981022	56447	345.260	1.560	58.633	0.012
981101	26940	346.143	2.571	61.551	0.180
		275.722	-23.305	44.973	0.085
981215	80709	301.383	-18.295	16.297	0.223
990109	41054	345.757	8.751	60.734	0.016
990110	31141	345.649	8.805	58.037	0.004
990128	37252	342.818	9.649	62.261	0.007
990204	30169	161.450	-9.832	73.846	0.169
990421	65775	146.070	-7.792	55.096	0.026
990509	74345	144.820	-7.244	81.947	0.375
990705	57685	147.515	-8.031	76.306	0.004
		167.925	-19.482	71.632	0.008
990707	54801	147.737	-8.132	56.409	0.010
990828	70019	155.115	-12.504	67.522	0.024
990919	49338	149.773	12.594	74.222	0.082
990926	32653	335.529	-9.725	14.580	1.019
991005	15265	340.866	17.520	18.198	0.110
991120	27069	198.957	-13.840	45.024	0.095
000102	27709	165.147	-34.791	51.204	0.236
000205	45486	156.800	-40.955	70.209	0.128
000206	09183	336.592	41.031	51.005	0.395
000403	13199	314.499	40.072	63.855	0.040
		308.246	19.750	46.194	0.167
000405	77386	133.665	-39.692	57.653	0.304

Table 2—Continued

Date	UT	$\alpha_{2000,IPN}$	$\delta_{2000,IPN}$	R_{IPN1}	δR_{IPN}
000420	61374	310.666	37.563	86.354	0.181
000511	66298	309.117	34.756	75.388	0.712

Table 3. *IPN error boxes*

Date	UT	α_{2000}	δ_{2000}	$\sigma_{sys+stat,B}$
910601	62220	297.900	8.300	2.330
		296.058	9.756	
		298.589	10.529	
		295.545	8.284	
		299.858	9.600	
910830	5148	202.100	14.700	2.130
		202.699	12.651	
		202.991	16.650	
		202.060	12.570	
		202.358	16.815	
910908	33924	230.800	-32.000	2.260
		230.053	-34.172	
		231.638	-29.857	
		229.842	-34.113	
		231.434	-29.806	
910910	14747	150.700	30.300	2.000
		148.384	30.285	
		152.795	31.170	
		148.393	30.134	
		152.864	31.031	
911029	17453	11.300	-18.700	2.130
		11.838	-20.769	
		13.048	-17.368	
		11.712	-20.794	
		12.966	-17.277	
911120	43957	74.300	35.100	3.050
		76.296	32.540	
		75.564	37.976	
		76.405	32.601	
		75.694	37.937	
920109	23306	345.500	33.800	11.410
		332.965	39.182	
		357.208	40.384	
		332.726	38.745	
		357.521	39.973	
920216	58688	322.900	18.200	2.260
		321.367	16.478	
		325.055	19.170	
		321.597	16.313	
		325.162	18.913	
920303	24523	318.400	-10.900	4.220
		318.255	-15.118	
		317.616	-6.752	
		318.434	-15.120	
		317.788	-6.724	
920622	23828	147.100	-39.400	2.720

Table 3—Continued

Date	UT	α_{2000}	δ_{2000}	$\sigma_{sys+stat,B}$
		148.636	-41.858	
		145.100	-41.656	
		149.203	-41.600	
		144.594	-41.337	
920626	64276	1.000	50.900	2.060
		0.000	0.000	
		0.000	0.000	
		0.000	0.000	
		0.000	0.000	
920717	57852	159.300	-71.600	2.000
		153.631	-72.582	
		165.497	-72.133	
		153.477	-72.483	
		165.564	-72.026	
920903	05728	299.100	28.800	1.890
		295.016	35.387	
		295.583	36.120	
		295.067	35.214	
		295.799	36.158	
930118	64426	219.200	-32.600	2.560
		220.633	-34.866	
		221.151	-30.652	
		220.541	-34.904	
		221.075	-30.599	
930209	15737	239.300	-58.200	1.750
		237.240	-59.590	
		237.460	-56.756	
		237.051	-59.508	
		237.272	-56.830	
930424	38888	230.100	-57.600	2.260
		233.507	-58.979	
		232.932	-55.956	
		231.473	-59.744	
		230.887	-55.382	
930506	55245	259.300	34.400	11.710
		252.549	24.267	
		253.061	45.092	
		254.773	23.377	
		256.039	45.844	
930626	07023	21.800	-40.200	10.320
		8.784	-43.846	
		21.353	-29.886	
		8.494	-42.978	
		20.326	-29.950	
930710	13810	316.500	-69.200	2.060
		322.028	-69.921	

Table 3—Continued

Date	UT	α_{2000}	δ_{2000}	$\sigma_{sys+stat,B}$
		310.697	-69.198	
		322.071	-69.873	
		310.705	-69.149	
930909	45100	244.000	9.400	2.000
		245.880	8.658	
		245.084	11.092	
		245.923	8.773	
		245.187	11.023	
940213	07260	191.900	-28.100	2.130
		194.111	-27.262	
		192.498	-26.038	
		194.303	-27.915	
		191.751	-25.974	
940222	8083	200.200	22.500	4.400
		203.083	19.022	
		195.460	23.007	
		202.862	18.872	
		195.441	22.750	
940311	44967	105.200	26.400	2.130
		0.000	0.000	
		0.000	0.000	
		103.541	27.936	
		105.460	28.518	
940710	35477	99.400	-33.300	3.760
		95.439	-35.148	
		98.463	-29.626	
		96.866	-36.433	
		100.452	-29.648	
940712	00070	66.700	-73.100	2.800
		66.982	-75.899	
		63.191	-70.522	
		67.472	-75.892	
		63.527	-70.480	
940727	40865	312.500	-1.900	2.260
		0.000	0.000	
		0.000	0.000	
		0.000	0.000	
		0.000	0.000	
940730	39690	79.700	-61.400	1.750
		83.263	-61.843	
		82.831	-60.531	
		0.000	0.000	
		0.000	0.000	
940930	23017	78.700	32.000	3.760
		74.499	30.863	
		81.554	34.911	

Table 3—Continued

Date	UT	α_{2000}	δ_{2000}	$\sigma_{sys+stat,B}$
		74.267	31.968	
		80.379	35.492	
941104	35178	345.300	18.500	5.920
		351.494	19.349	
		340.023	21.742	
		351.427	19.743	
		340.265	22.072	
950111	46528	24.300	-5.800	1.790
		25.708	-6.916	
		23.085	-4.481	
		25.546	-7.092	
		22.919	-4.654	
950131	78592	319.400	-58.800	6.790
		332.034	-61.367	
		307.773	-56.126	
		332.489	-60.312	
		308.789	-55.212	
950203	08456	274.600	42.700	2.000
		273.162	41.011	
		276.802	43.897	
		273.232	40.979	
		276.851	43.846	
950211	15919	325.600	3.300	1.750
		323.883	2.949	
		327.178	4.064	
		323.955	2.698	
		327.274	3.822	
950611	21122	269.800	-69.500	2.480
		0.000	0.000	
		0.000	0.000	
		0.000	0.000	
		0.000	0.000	
950615	12104	310.200	-48.500	6.110
		317.991	-52.050	
		302.386	-45.503	
		316.943	-52.875	
		301.692	-46.428	
950622	71470	213.400	-1.500	4.680
		216.922	1.582	
		210.342	2.043	
		217.169	1.275	
		210.055	1.773	
950722	64127	74.200	25.800	3.580
		78.163	25.551	
		70.224	25.950	
		78.144	26.310	

Table 3—Continued

Date	UT	α_{2000}	δ_{2000}	$\sigma_{sys+stat,B}$
950730	76147	70.337	26.703	
		218.300	-13.400	2.193
		216.499	-14.090	
		220.702	-13.533	
		216.511	-14.168	
950904	52777	220.711	-13.611	
		197.100	33.300	2.190
		196.048	31.299	
		198.492	31.452	
		195.522	31.561	
951001	41868	198.968	31.778	
		127.100	-0.300	2.970
		129.732	1.076	
		126.889	2.663	
		129.600	1.304	
951112	67850	127.153	2.670	
		225.700	16.900	1.940
		223.970	15.896	
		227.667	16.437	
		223.782	16.281	
951124	25132	227.727	16.858	
		157.300	47.600	2.190
		157.526	45.416	
		154.289	48.462	
		160.092	46.514	
951218	28745	156.796	49.765	
		20.700	-20.700	2.000
		19.312	-22.227	
		22.801	-21.085	
		19.491	-22.354	
960115	31956	22.748	-21.288	
		132.300	-50.200	4.030
		137.695	-52.409	
		127.935	-47.375	
		137.535	-52.562	
960201	82195	127.746	-47.504	
		170.700	-15.600	6.400
		177.126	-17.328	
		164.395	-13.665	
		177.042	-17.609	
960202	05968	164.306	-13.944	
		104.400	54.600	2.060
		107.037	53.246	
		100.892	54.993	
		107.379	53.511	
		101.036	55.318	

Table 3—Continued

Date	UT	α_{2000}	δ_{2000}	$\sigma_{sys+stat,B}$
960207	65033	9.800	35.800	2.260
		8.257	33.928	
		12.029	34.464	
		8.022	34.072	
		12.193	34.665	
960304	48776	72.800	23.400	3.050
		75.184	21.292	
		69.613	22.567	
		75.734	21.995	
		69.476	23.427	
961017	23648	162.800	42.400	4.030
		157.992	40.590	
		164.912	46.136	
		158.495	40.001	
		165.805	45.805	
961209	74677	188.600	33.400	5.630
		188.241	27.778	
		184.992	38.211	
		183.130	30.222	
		181.856	33.794	
961213	49966	186.300	57.300	2.720
		189.274	55.140	
		181.933	56.019	
		188.793	54.961	
		182.254	55.744	
970116	58238	181.300	-49.300	2.560
		178.432	-51.084	
		184.499	-50.830	
		178.071	-50.803	
		184.795	-50.520	
970406	25471	287.300	-28.200	4.120
		284.199	-31.319	
		287.704	-24.096	
		284.742	-31.673	
		288.335	-24.186	
970801	29048	311.600	-54.200	2.260
		312.760	-56.361	
		307.838	-53.740	
		313.585	-56.156	
		308.119	-53.267	
971027	09808	194.600	67.500	1.630
		0.000	0.000	
		0.000	0.000	
		0.000	0.000	
		0.000	0.000	
971101	23483	359.000	13.100	1.840

Table 3—Continued

Date	UT	α_{2000}	δ_{2000}	$\sigma_{sys+stat,B}$
		0.531	12.026	
		357.113	13.202	
		0.513	12.003	
		357.112	13.173	
971121	43992	288.000	-71.000	3.310
		0.000	0.000	
		0.000	0.000	
		0.000	0.000	
		0.000	0.000	
971207	67900	91.200	56.000	5.150
		89.818	50.916	
		89.893	61.105	
		90.537	50.865	
		90.833	61.146	
971207	75492	131.400	71.100	5.540
		125.571	65.980	
		148.573	72.644	
		125.820	65.945	
		148.619	72.537	
971228	79012	50.600	-58.100	3.580
		56.348	-60.131	
		44.681	-56.488	
		0.000	0.000	
		0.000	0.000	
980205	19783	146.400	-37.400	2.449
		141.408	-36.889	
		149.002	-39.630	
		141.537	-36.855	
		149.169	-39.591	
980523	31208	336.100	-50.600	5.440
		328.652	-48.129	
		341.734	-46.631	
		328.989	-47.767	
		341.252	-46.362	
980622	51085	247.000	-49.900	5.350
		248.967	-55.115	
		249.002	-44.724	
		249.068	-55.100	
		249.083	-44.739	
980629	32377	271.700	53.600	1.840
		270.855	51.833	
		273.931	54.899	
		270.917	51.822	
		273.978	54.870	
980812	18950	337.300	33.900	3.140
		340.558	32.346	

Table 3—Continued

Date	UT	α_{2000}	δ_{2000}	$\sigma_{sys+stat,B}$
980913	19983	333.941	32.499	
		340.474	32.231	
		334.018	32.381	
		10.800	6.500	3.580
		12.306	3.250	
		10.380	10.056	
981019	79603	11.775	3.054	
		9.818	9.945	
		318.700	-36.700	3.220
		322.038	-38.539	
		315.772	-34.531	
		322.079	-38.490	
981022	56447	315.821	-34.489	
		287.900	8.000	6.110
		286.585	2.032	
		287.253	14.077	
		286.609	2.027	
		287.278	14.079	
981101	26940	290.700	18.400	2.260
		285.480	20.739	
		285.453	20.570	
		285.856	20.658	
		285.829	20.489	
		298.000	-2.800	2.720
981215	80709	295.278	-2.895	
		300.530	-1.796	
		295.333	-3.352	
		300.663	-2.236	
		319.500	-49.200	1.940
		322.111	-48.305	
990109	41054	319.282	-47.265	
		322.068	-48.254	
		319.369	-47.262	
		287.100	9.700	3.223
		287.081	6.477	
		286.582	12.883	
990110	31141	287.088	6.477	
		286.589	12.884	
		304.900	-41.900	1.680
		306.488	-43.105	
		303.203	-40.804	
		306.503	-43.094	
990204	30169	303.216	-40.793	
		131.600	63.200	3.490
		130.012	59.793	
		138.763	62.040	

Table 3—Continued

Date	UT	α_{2000}	δ_{2000}	$\sigma_{sys+stat,B}$
		131.050	59.720	
		138.262	61.569	
990421	65775	93.000	-44.000	2.640
		0.000	0.000	
		0.000	0.000	
		0.000	0.000	
		0.000	0.000	
990509	74345	234.000	-25.300	7.280
		230.251	-31.794	
		229.206	-19.522	
		229.333	-31.312	
		228.459	-20.114	
990705	57685	79.100	-72.300	1.750
		77.451	-72.112	
		77.488	-72.150	
		77.460	-72.090	
		77.497	-72.127	
990707	54801	102.700	-53.000	1.840
		105.730	-53.289	
		103.292	-51.196	
		105.736	-53.261	
		103.336	-51.202	
990828	70019	221.000	-66.600	2.560
		215.426	-67.990	
		219.021	-64.176	
		215.346	-67.937	
		218.889	-64.195	
990919	49338	69.400	74.000	2.720
		71.601	71.360	
		74.556	76.382	
		72.134	71.404	
		75.176	76.285	
990926	32653	350.600	-6.100	3.760
		351.358	-9.784	
		349.452	-2.518	
		349.287	-9.628	
		347.741	-3.646	
991005	15265	329.000	37.900	1.840
		0.000	0.000	
		0.000	0.000	
		0.000	0.000	
		0.000	0.000	
991120	27069	153.400	-28.700	2.060
		153.311	-30.759	
		152.564	-26.777	
		153.536	-30.757	

Table 3—Continued

Date	UT	α_{2000}	δ_{2000}	$\sigma_{sys+stat,B}$
000102	27709	152.770	-26.717	
		213.200	-13.900	2.720
		0.000	0.000	
		0.000	0.000	
		0.000	0.000	
		0.000	0.000	
000205	45486	203.000	14.600	2.000
		204.808	13.637	
		201.462	15.941	
		204.665	13.421	
		201.297	15.740	
		28.100	18.200	2.130
000206	09183	29.289	16.398	
		30.195	17.451	
		27.932	16.076	
		30.257	18.792	
		275.100	-10.700	1.710
		272.977	-10.966	
000403	13199	274.144	-11.737	
		272.758	-10.720	
		273.909	-11.487	
		226.900	-52.500	2.640
		0.000	0.000	
		0.000	0.000	
000420	61374	0.000	0.000	
		0.000	0.000	
		104.100	54.200	1.840
		102.483	52.632	
		107.083	53.652	
		101.930	52.887	
000511	66298	107.232	54.064	
		48.700	38.000	2.260
		47.337	36.019	
		50.491	39.779	
		46.089	37.093	
		48.679	40.260	